the FEBS Journal

Interaction of synthetic peptides corresponding to hepatitis G virus (HGV/GBV-C) E2 structural protein with phospholipid vesicles

Cristina Larios[1,2], Bart Christiaens[3], M. José Gómara[1], M. Asunción Alsina[2] and Isabel Haro[1]

1 Department of Peptide and Protein Chemistry, IIQAB-CSIC, Barcelona, Spain
2 Associated Unit CSIC, Department of Physical Chemistry, Faculty of Pharmacy, University of Barcelona, Spain
3 Laboratory of Lipoprotein Chemistry, Department of Biochemistry, Ghent University, Belgium

Keywords
circular dichroism; fluorescence assays; hepatitis G virus (HGV/GBV-C); lipid vesicles; synthetic peptides

Correspondence
I. Haro, Department of Peptide and Protein Chemistry, IIQAB-CSIC, Jordi Girona 18-26 08034, Barcelona, Spain
Fax: +34 9320 45904
Tel: +34 9340 06109
E-mail: ihvqpp@iiqab.csic.es

(Received 25 February 2005, revised 8 March 2005, accepted 17 March 2005)

doi:10.1111/j.1742-4658.2005.04666.x

The interaction with phospholipid bilayers of two synthetic peptides with sequences corresponding to a segment next to the native N-terminus and an internal region of the E2 structural hepatitis G virus (HGV/GBV-C) protein [E2(7–26) and E2(279–298), respectively] has been characterized. Both peptides are water soluble but associate spontaneously with bilayers, showing higher affinity for anionic than zwitterionic membranes. However, whereas the E2(7–26) peptide is hardly transferred at all from water to the membrane interface, the E2(279–298) peptide is able to penetrate into negatively charged bilayers remaining close to the lipid/water interface. The nonpolar environment clearly induces a structural transition in the E2(279–298) peptide from random coil to α-helix, which causes bilayer perturbations leading to vesicle permeabilization. The results indicate that this internal segment peptide sequence is involved in the fusion of HGV/GBV-C to membrane.

The hepatitis G virus (HGV) and the GB virus C (GBV-C) are strain variants of a recently discovered enveloped RNA virus belonging to the Flaviviridae family, which is transmitted by contaminated blood and/or blood products, intravenous drug use, from mother to child and by sexual intercourse. The natural history of HGV/GBV-C infection is not fully understood, and its potential to cause hepatitis in humans is questionable [1]. Moreover, the mode of entry of HGV/GBV-C into target cells is not known.

Elucidation of the mechanism of the fusion of enveloped viruses with target membranes has attracted considerable attention because of its relative simplicity and potential clinical importance. Apart from the functions of viral binding to target membranes and the activation of viral fusion proteins, usually only one viral protein is responsible for the actual membrane fusion step. However, the nature of the interaction of viral fusion proteins with membranes and the mechanism by which these proteins accelerate the formation of membrane fusion intermediates are poorly understood [2]. In this sense, specialized hydrophobic conserved domains ('fusion peptides') have been postulated to be absolutely required for the fusogenic activity [3,4].

The envelope proteins (E) of flaviviruses have been described as class II fusion proteins that have structural features that set them apart from the well-known rod-like 'spikes' of influenza virus or HIV. They are predominantly nonhelical, having instead a β-sheet-type

Abbreviations
E, envelope proteins; HCV, hepatitis C virus; HGV/GBV-C, hepatitis G virus; LUV, large unilamellar vesicle; PamOlePtdCho, 1-palmitoyl-2-oleoylphosphatidylcholine; PamOlePtdGro, 1-palmitoyl-2-oleoylphosphatidylglycerol; SUV, small unilamellar vesicle; TBEV, tick-borne encephalitis virus.

structure; they are not cleaved during biosynthesis and appear to have fusion peptides within internal loop structures, distant from the N-terminus [5]. The only protein of this class for which a high-resolution structure is available is the envelope glycoprotein E of the flavivirus tick-borne encephalitis virus (TBEV) [6]. It has been proposed that a highly conserved loop at the tip of each subunit of the flavivirus E protein (sequence element containing amino acids 98–110 of the flavivirus E protein) may serve as an internal fusion peptide, as it is directly involved in interactions with target membranes during the initial stages of membrane fusion [7]. Because of the structural homology, extrapolating knowledge from the TBEV structure to hepatitis C virus (HCV) leads to the idea that E2 may be the fusion protein. Although very little is known about the HCV cell fusion process, sequence alignment between the TBEV E protein and the HCV E2 protein suggests that residues 476–494 in E2 may play a role in viral fusion [8]. As HGV/GBV-C is the most closely related human virus to HCV [9], it can be expected that E2 sequences of these related viruses are functionally equivalent, and therefore conserve some structural similarity. However, owing to the low pairwise sequence identity with HCV E2 (< 20%), attempts to align these sequences using sequence information and/or through their predicted secondary structure have been unsuccessful and have given ambiguous results [8].

Besides, experimental information on the type of interactions established by internal fusion peptides with membranes is at present limited. Predictive structural analyses indicate that internal fusion peptides are segmented into two regions separated by a putative turn or loop, which usually contains one or more Pro residues. This organization seems to be fundamental to the fusogenic function [10]. It has been shown that Pro residues display the highest propensity for turn induction at the membrane interface in poly(Leu) stretches [11,12] and therefore play important structural roles in membrane-inserted peptide chains [13].

The direct involvement of fusion peptides in virus–cell fusion is supported by studies using model membranes, membrane mimetic systems, and synthetic peptide fragments representing functional and nonfunctional fusion peptide sequences, which demonstrate that, after insertion, only functional sequences generate target-membrane perturbations [4].

In this study, we report on the interaction of an N-terminal (E2(7–26)) and an internal (E2(279–298)) synthetic peptide sequence of the E2 structural protein of HGV/GBV-C with phospholipid membranes of different composition. To select these peptides, the profiles of Kite and Doolittle (hydropathicity index) and Chou and Fasman (secondary-structure prediction) were used to determine E2 regions sharing both partition into membranes and β-turn structure tendencies. In this sense, the two selected E2 regions, in spite of having Pro within their primary sequences, showed different features. Thus, whereas E2(7–26) has a high β-turn content but no membrane affinity, the region of E2 located between residues 279 and 298 has both predictive features.

The secondary structure of both peptides was measured by CD. We monitored several parameters that determine peptide–membrane interaction, and combined analysis of the data obtained provides insights into HGV/GBV-C–membrane interaction.

Results

The E2 peptides synthesized are amphiphilic because of the presence of hydrophobic and hydrophilic amino acids in their composition which make them water soluble and able to associate with model membranes. E2(7–26) (GSRPFEPGLTWQSCSCRANG) contains two positively charged Arg residues (Arg9 and Arg23), which could be important for the interaction with negatively charged phospholipid membranes [14]. E2(279–298) (AGLTGGFYEPLVRRCSELAG) is a neutral peptide containing two positive arginines (Arg285, Arg286) and two negatively charged amino acids (Glu282, Glu290); it has an isoelectric point (pI) of 6.18 and a mean hydrophobicity (H_0) of 0.13.

A Trp residue was incorporated at the N-terminus of the wild E2(279–298) sequence to provide a suitable chromophore for monitoring lipid–peptide interaction. The presence of this Trp residue in W-E2(279–298) modified neither the hydrophobicity (0.16) nor the pI (6.14) of the parent E2(279–298) peptide.

Binding of E2 peptides to model membranes

Lipid interaction of the E2 peptides was studied by monitoring Trp fluorescence changes on titration of peptide solutions with small unilamellar vesicles (SUVs).

In Tris/HCl buffer containing 150 mM NaCl, the maximal Trp fluorescence emission wavelength (λ_{max}) of the peptides was 347 and 350 nm for E2(7–26) and W-E2(279–298), respectively. Our results show that, in lipid-free peptides, Trp residues are highly exposed to water.

To investigate the contribution of electrostatic interactions, the peptides were titrated with both neutral and negatively charged vesicles. Titration of the

peptides with neutral 1-palmitoyl-2-oleoylphosphatidylcholine (PamOlePtdCho) SUVs resulted in no shift for E2(7–26) and a shift of only 1 nm for W-E2(279–298).

Incubation of E2(7–26) peptide with negatively charged vesicles, PamOlePtdCho/1-palmitoyl-2-oleoylphosphatidylglycerol (PamOlePtdGro) (75/25) and egg PtdCho/brain PtdSer (65/35), had little effect on the Trp fluorescence intensity of the peptide and did not affect the shape of the Trp fluorescence spectrum. Blue shifts of 3 nm and 1 nm were found for this peptide upon titration with 200 μM PamOlePtdCho/PamOlePtdGro (75/25) and 200 μM PtdCho/PtdSer (65/35). In contrast, addition of the negatively charged vesicles to the E2(279–298) peptide shifted the maximal Trp fluorescence emission to lower wavelengths. The larger blue shift of 11 nm was measured for the peptide titration with egg PtdCho/brain PtdSer (65/35). Blue shifts of this magnitude have been observed when surface-active Trp-containing peptides interact with lipid membranes and are consistent with the Trp residue partition into a more hydrophobic environment [15–19]. This also indicates that the Trp residues are only partially buried in the vesicles, as a moiety that is fully protected from water is expected to have emission at $\approx$320 nm.

As a general rule, on titration with negatively charged vesicles, Trp fluorescence decreased and the wavelength of maximal Trp fluorescence shifted to lower wavelengths. As an example, Fig. 1 shows the curves of the peptides in buffer and in the presence of PamOlePtdCho/PamOlePtdGro SUVs.

The electrostatic interactions were further studied by titration of the peptides with egg PtdCho/brain PtdSer (65/35) SUVs in Tris/HCl buffer without salt. For both peptides, the blue shift increased up to 14 and 15 nm for E2(7–26) and W-E2(279–298), respectively.

After titration with egg PtdCho/brain PtdSer (65/35) SUVs without salt, the blue shift was also accompanied by a decrease in the Trp fluorescence intensity. Plotting the percentage of initial fluorescence as a function of the lipid concentration (Fig. 2) enabled calculation of K_d values. For both peptides, the titration curves show saturable binding. The affinity for egg PtdCho/brain PtdSer (65/35) SUVs was higher for W-E2(279–298) than for E2(7–26) [K_d was 67 ± 10 μM for E2(7–26) and 31 ± 2.5 μM for W-E2(279–298)] (Table 1).

Finally, the effect of membrane rigidity was studied using PamOlePtdCho/PamOlePtdGro/cholesterol (45/30/25) SUVs. The presence of cholesterol in the lipid bilayer had a minor effect, as there was a shift in λ_{max} of 3 nm for E2(7–26) and 6 nm for W-E2(279–298).

Peptide conformation

In buffer, the CD spectra for the E2 peptides showed the characteristics of a random-coil conformation, as indicated by the presence of a negative band at

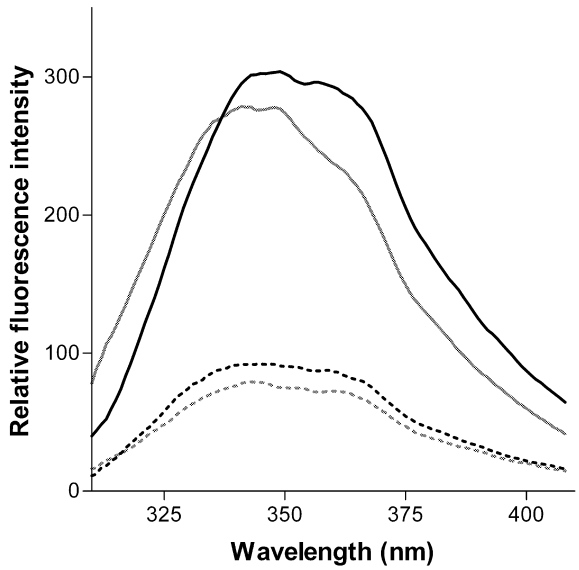

Fig. 1. Fluorescence emission spectra of the E2(7–26) (black broken line) and W-E2(279–298) (black solid line) peptides (2 μM) in Tris/HCl buffer (pH 8)/0.15 mM NaCl (black) and in the presence of 0.2 mM PamOlePtdCho/PamOlePtdGro (75/25) SUVs (grey).

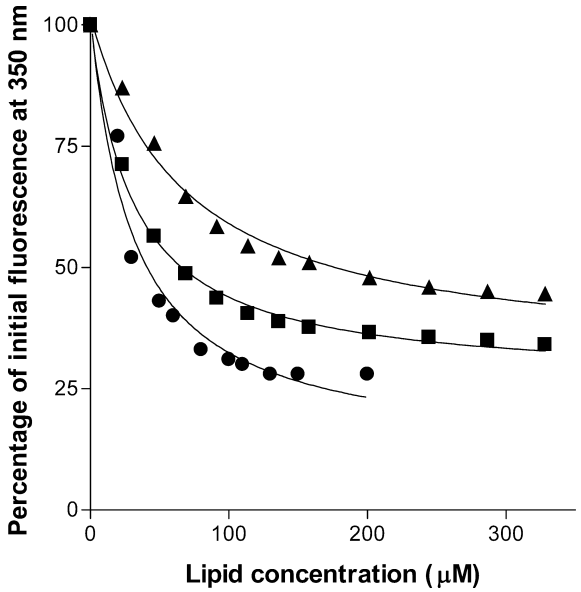

Fig. 2. Fluorescence titration curves of E2(7–26) (▲), W-E2(279–298) (■) and penetratine(43–58) (●) with egg PtdCho/brain PtdSer (65/35) SUVs without salt. Curve-fitting of the experimental data is represented by solid lines.

Table 1. Maximal Trp emission wavelength (λ max) for lipid-free and lipid-bound E2(7–26), W-E2(279–298) and P(48–53) peptides, apparent dissociation constants (K_d) for titration of the peptides with egg PtdCho/brain PtdSer (65/35) SUVs, and Stern–Volmer constants (K_{sv}) for acrylamide quenching of Trp fluorescence of the peptides before and after incubation with egg PtdCho/brain PtdSer (60/40) SUVs. P(43–58), Penetratine(43–58).

	E2(7–26)	W-E2(279–298)	P(43–58)
λ_{max} (nm)			
Buffer	347	350	347
PamOlePtdCho	347	349	347
PamOlePtdCho/PamOlePtdGro (75/25)	344	342	337
PamOlePtdCho/PamOlePtdGro/Chol (45/30/25)	344	344	339
Egg PtdCho/brain PtdSer (65/35)	346	339	338
Egg PtdCho/brainPS buffer no salt (65/35)	332	336	339
K_d (μM)			
Egg PtdCho/brain PtdSer (65/35)	67 ± 10	31 ± 2.5	5.5 ± 0.1
K_{sv} (M^{-1})			
Buffer	13.6 ± 0.6	26.6 ± 0.2	18.6 ± 1.1
Egg PtdCho/brain PtdSer (60/40)	6.8 ± 0.2	7.2 ± 0.2	2.7 ± 0.1

198 nm. In aqueous 2,2,2-trifluoroethanol solutions, the percentage of α-helix in W-E2(279–298) increased, whereas this was not the case for E2(7–26). In Fig. 3, as an example, the CD spectra of E2 (279–298) in buffer, in 50% (v/v) trifluoroethanol, and in PamOlePtdCho/PamOlePtdGro (2 : 1) SUVs are shown. We can observe the change to a more structured conformation when the mimetic membrane solvent trifluoroethanol or SUVs are added.

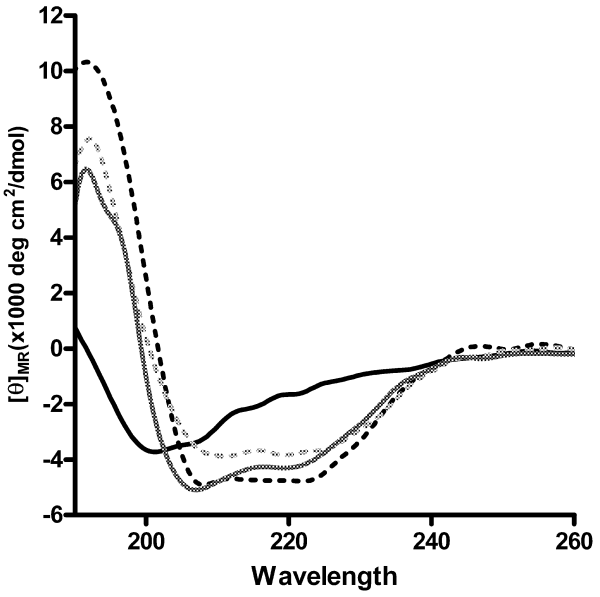

Fig. 3. CD spectra of W-E2(279–298) (22 μM) in phosphate buffer, pH 7.4 (black solid line), 50% trifluoroethanol (black broken line) and PamOlePtdCho/PamOlePtdGro (80/20) SUVs (grey broken line). CD spectrum of penetratine(43–58) in PamOlePtdCho/PamOlePtdGro (80/20) SUVs (grey solid line).

Incubation with mixed PamOlePtdCho/PamOlePtdGro (80/20) or PamOlePtdCho/PamOlePtdGro/cholesterol (50/25/25) SUVs increased the α-helix content of W-E2(279–298) (Table 2). In contrast, the percentage of β-type structure decreased. In all cases, E2(7–26) remained mainly unstructured, even when bound to phospholipid vesicles.

Acrylamide quenching

The accessibility of the Trp residues of the E2 peptides to the neutral, water-soluble acrylamide quencher was examined in the absence and presence of phospholipid vesicles. Fluorescence of Trp decreased in a concentration-dependent manner after the addition of acrylamide to the peptide solution in the presence or absence of liposomes (data not shown). Figure 4 shows the Stern-Volmer plots for acrylamide quenching of E2 peptides in buffer, and in the presence of egg PtdCho/brain PtdSer (60/40) SUV vesicles. The Stern-Volmer quenching constants (K_{sv}) of the lipid-free peptides were 13.6 ± 0.6 M^{-1} for E2(7–26) and 26.6 ± 0.2 M^{-1} for W-E2(279–298) (Table 1), indicating that the Trp residue of the peptides was readily quenched by acrylamide. Incubation with egg PtdCho/brain PtdSer (60/40) SUVs decreased the K_{sv} values twofold for E2(7–26) and 3.7-fold for W-E2(279–298), showing in the latter case that the Trp residues are more protected from the quencher.

Quenching by brominated lipids

The depth of insertion of the Trp residues of E2 peptides into lipid bilayers was estimated by dibromo-PtdCho

Table 2. α-Helical, β-structure and random coil content of the E2 peptides, as calculated using the K2D and CONTIN programs, and based on the mean residue ellipiticity at 222 nm [33]. TFE, trifluoroethanol.

	% α-Helix			% β-Structure			% Random oil	
	θ_{222}	K2D	CONTIN	β-Sheet (K2D)	β-Sheet (K2D)	β-Turn (CONTIN)	K2D	CONTIN
E2(7–26)								
Buffer	13	8	12	41	27	24	50	37
25% TFE	15	9	12	36	32	22	55	34
50% TFE	18	14	16	30	29	23	42	33
PamOlePtdCho	11	7	9	51	34	23	50	36
PamOlePtdCho/PG (80/20)	15	8	11	41	31	22	50	36
PamOlePtdCho/PG/Chol (50/25/25)	15	8	4	41	44	18	56	32
E2(279–298)								
Buffer	15	10	13	34	16	16	56	55
25% TFE	33	10	14	36	17	14	55	55
50% TFE	34	28	37	15	14	16	58	33
PamOlePtdCho	20	33	37	16	20	14	50	28
PamOlePtdCho/PG (80/20)	28	46	42	20	15	16	33	27
PamOlePtdCho/PG/Chol (50/25/25)	29	57	47	10	17	16	33	19

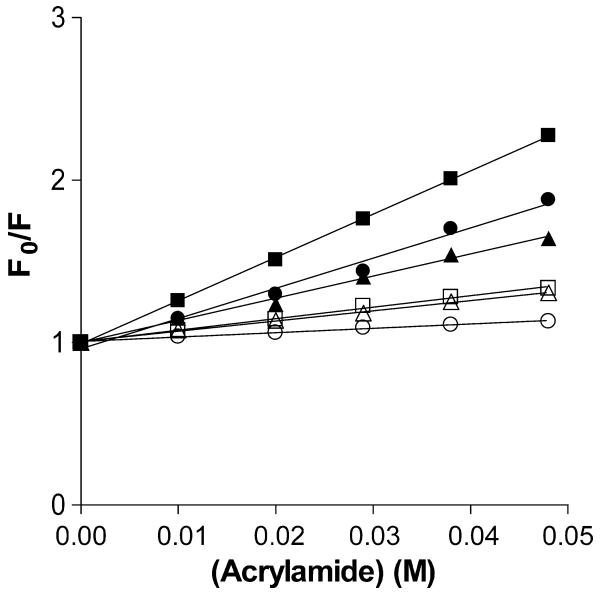

Fig. 4. Stern–Volmer plots for acrylamide quenching of E2(7–26) (triangles), W-E2(279–298) (squares) and penetratine(43–58) (circles). Filled symbols represent the peptides in aqueous buffer; open symbols represent the peptides in the presence of 0.2 mM egg PtdCho/brain PtdSer (60/40) SUVs.

quenching. Both peptides were quenched more efficiently by $Br_{6,7}$-PtdCho than by $Br_{11,12}$-PtdCho (Fig. 5), suggesting that they remain close to the lipid/water interface. For both lipid quenchers, Trp quenching efficiency was higher for W-E2(279–298) than for E2(7–26), indicating deeper insertion of W-E2(279–298) into the membrane.

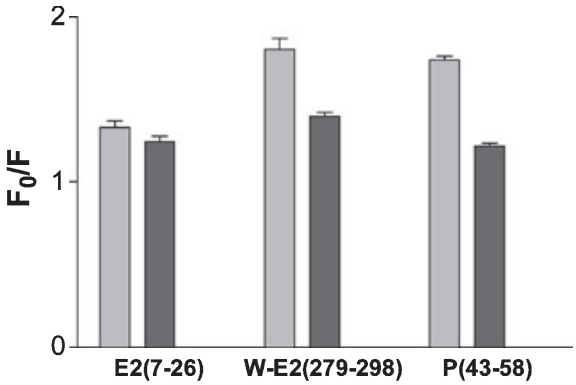

Fig. 5. Trp quenching efficiency (F_0/F) of E2(7–26), W-E2(279–298) and penetratine(43–58) peptides (2 μM) bound to egg PtdCho/brain PtdSer (65/35) SUVs (lipid to peptide molar ratio 0.01) by $Br_{6,7}$-PtdCho (grey bars) and $Br_{11,12}$-PtdCho (black bars).

Membrane permeabilization

Figure 6 shows the calcein leakage out of egg PtdCho/brain PtdSer (70 : 30) large unilamellar vesicles (LUVs) induced by the E2 peptides. Leakage of 70% was reached for E2(7–26) at a peptide to lipid ratio of 2 : 1. For W-E2(279–298), complete lysis of the LUVs was reached at a peptide to lipid ratio of 1 : 1. For the E2(7–26) peptide, a sigmoidal dose–response curve was obtained, indicating peptide co-operativity, whereas this was not the case for W-E2(279–298) (Fig. 6A). Calcein leakage kinetics were faster for the W-E2(279–298) peptide, which induced complete vesicle lysis after 15 min compared with 1 h for the E2(7–26) peptide (Fig. 6B).

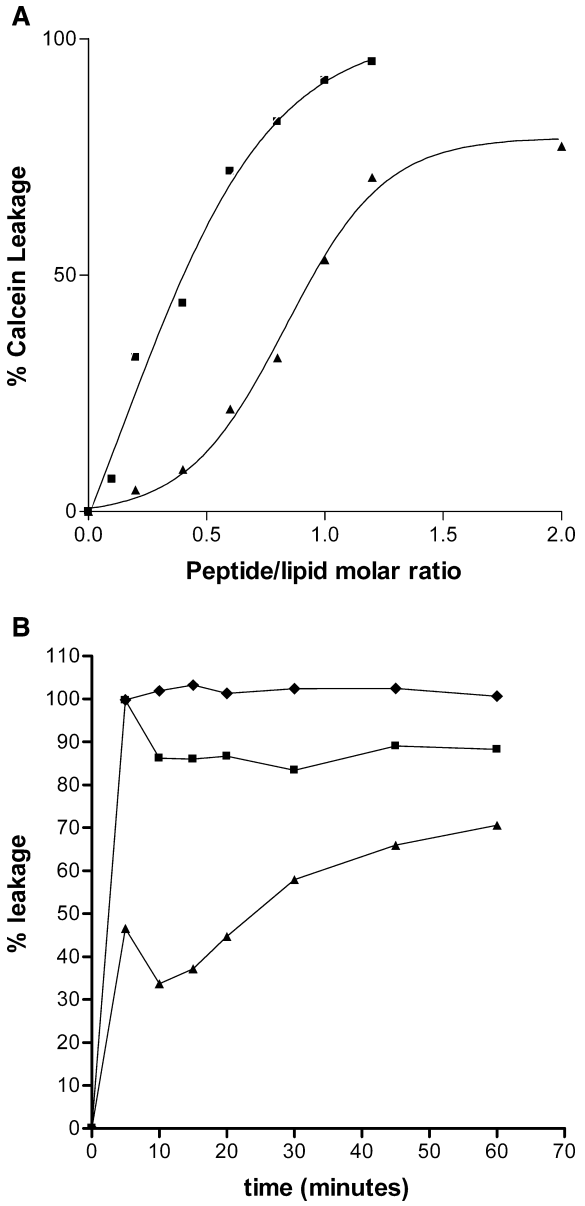

Fig. 6. (A) Calcein leakage induced by E2(7–26) (▲) and W-E2(279–298) (■) from egg PtdCho/brain PtdSer (70/30) LUVs as a function of peptide to lipid molar ratio. (B) Percentage of leakage vs. time for E2(7–26) (▲), W-E2(279–298) (■), and melittin (●). Peptide to lipid molar ratio 1 : 1 (E2 peptides) and 1 : 25 (melittin).

Vesicle aggregation

Incubation of egg PtdCho/brain PtdSer (60/40) SUVs with E2(7–26) peptide induced vesicle aggregation at a 0.2 peptide to lipid ratio, as indicated by the increase in A_{436} (Fig. 7). In contrast, the W-E2(279–298) peptide did not show any increase in A_{436}.

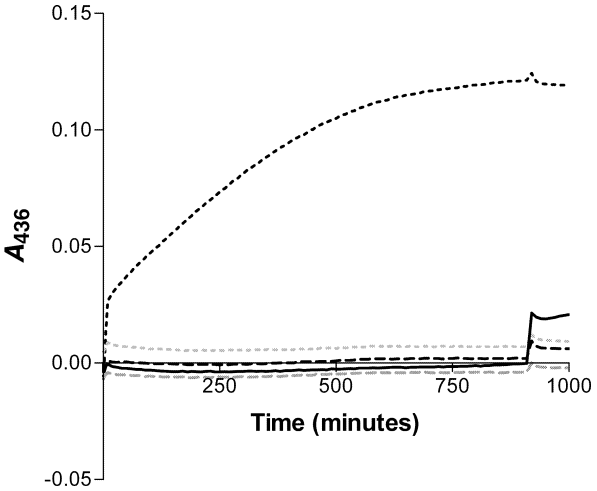

Fig. 7. Turbidity (A_{436}) of dispersion of egg PtdCho/brain PtdSer SUVs in the absence (solid line) and presence of the E2(7–26) (black) and W-E2(279–298) (grey) peptides at 0.04 (broken line) and 0.2 (dotted line) peptide to lipid molar ratio.

Discussion

HGV/GBV-C is the most closely related human virus to HCV, both of them belonging to the small enveloped viruses of the Flaviviridae family. A stretch of conserved, hydrophobic amino acids within the E2 envelope glycoprotein of HCV has been proposed as the virus fusion peptide [8]. However, because of the low pairwise sequence identity with HCV E2 ($< 20\%$), it has not been feasible to select a stretch of residues in the HGV/GBV-C E2 protein, with sequence homology to the highly conserved loop of the flavivirus E protein described as an internal fusion peptide.

In this study we have analysed the interactions of an N-terminal and an internal peptide sequence of the E2 structural protein of HGV/GBV-C with model membranes, in order to understand the possible mode of penetration of HGV/GBV-C into the membrane cells. These synthetic peptides are characterized by the presence of Pro residues, which have been reported to play important roles in membrane-inserted peptide chains, specifically promoting kinks at the level of the membrane interface. Moreover, they have a high content of aliphatic hydrophobic residues, such as Val and Leu, and aromatic hydrophobic residues (Tyr, Phe, Trp), as well as the three small amino acids Gly, Ala, Thr. It has been suggested that these particular amino-acid contents may confer structural plasticity on these peptides, which seems to be crucial for the fusion process [20].

Although fusion peptides have been widely described as short hydrophobic segments of viral envelope glycoproteins with a very low content of hydrophilic amino acids, the presence of acidic residues in the fusion peptides of some low-pH-activated viral fusion proteins has been observed [21]. Moreover, it has been reported that the putative internal fusion peptide of TBEV is highly constrained by multiple interactions, including several internal hydrogen bonds and salt bridges [22]. The analogue fusion peptide proposed for HCV is characterized by a positively charged region, which has been shown experimentally to be important for heteromeric association between envelope proteins E1 and E2 [8]. Therefore, the presence of hydrophilic amino acids in the fusion peptides of flaviviruses seems to be crucial for the fusion process.

We have investigated the fluorescence properties of the Trp residues of E2(7–26) and W-E2(279–298) peptides in buffer as well as in the presence of neutral and negatively charged vesicles. In lipid-free peptides, both Trp residues are highly exposed to the aqueous phase, suggesting a monomeric rather than aggregated structure. This was confirmed by the extent of acrylamide quenching. Moreover, CD measurements showed that both peptides are randomly structured in buffer.

The addition of neutral lipid vesicles to the peptides induced no blue shift of λ_{max}, suggesting that the peptides hardly interacted at all with PamOlePtdCho SUVs. The E2(7–26) peptide titration with negatively charged vesicles [PamOlePtdCho/PamOlePtdGro (75/25) and PtdCho/PtdSer (65/35)] showed a slight blue shift in Trp fluorescence, suggesting a weak interaction between this sequence and negatively charged SUVs. In contrast, W-E2(279–298) strongly interacted with PtdCho/PtdSer (65/35) vesicles, as the blue shift of Trp was 11 nm.

To study the contribution of electrostatic interactions to the binding of both peptides with negatively charged SUVs, titration of the peptides with PtdCho/PtdSer vesicles was carried out in the absence of salt. The E2(7–26) peptide showed a significantly higher blue shift of Trp fluorescence in buffer without salt, whereas W-E(279–298) showed a similar fluorescence spectrum to that obtained in 10 mM Tris/HCl buffer containing 0.15 M NaCl. These results suggest that electrostatic interactions play a principal role in the binding of E2(7–26) to negatively charged residues. In contrast, a higher contribution of hydrophobic compared with electrostatic interactions is expected to control the binding of W-E2(279–298) to PtdCho/PtdSer vesicles. This is supported by the vesicle aggregation results induced on the addition of peptides to PtdCho/PtdSer (60/40) SUVs. Thus, in contrast with W-E2(279–298) peptide, the E2(7–26) sequence promoted vesicle aggregation, confirming that the binding of this peptide to PtdCho/PtdSer vesicles is mainly due to electrostatic interactions.

Acrylamide and dibromo-PtdCho quenching experiments were performed to estimate the depth of insertion of the Trp residues of E2 peptides into lipid bilayers. The Stern-Volmer quenching constants for the PtdCho/PtdSer-incubated peptides, as well as the Trp quenching efficiency by brominated lipids, indicated a deeper insertion of W-E2(279–298) into the membrane than E2(7–26) peptide. Moreover, $Br_{6,7}$-PtdCho quenched the Trp residue in W-E2(279–298) more efficiently than $Br_{11,12}$-PtdCho, suggesting that this peptide remains close to the lipid/water interface.

Cell membranes have an asymmetric distribution of zwitterionic and negatively charged phospholipids characterized by localization in the inner leaflet of the bilayer of the second one. In a previous study [14], it has been suggested that the preferential interaction of the synthetic peptides with anionic membranes may be related to the fact that some membrane proteins, having clusters of basic amino acids, require small amounts of anionic lipids to interact with the cell membrane.

Induction of vesicle permeability on addition of peptide fragments representing fusion peptide sequences has been shown to correlate well with fusion peptide functionality, in most instances. In this study, we compared the ability of E2(7–26) and W-E2(279–298) to induce leakage from PtdCho/PtdSer (70 : 30) vesicles. The calcein release induced by the peptides was dependent on the concentration, so when a sufficient high concentration of the peptides is reached, a larger aggregated form could induce the membrane permeability. The W-E2(279–298) peptide showed significantly higher leakage activity than E2(7–26), as the former was able to induce extensive efflux of aqueous contents into the medium at a peptide to lipid molar ratio two times lower. This vesicle permeabilization process appears to be mediated by the peptide conformation adopted in membranes. CD experiments showed that the addition of 50% trifluoroethanol or negatively charged vesicles induced α-helical conformation in the W-E2(279–298) peptide. However, the E2(7–26) peptide conformation in a membraneous environment remained random coil like.

The data together suggest that the E2(7–26) peptide is hardly transferred at all from water to the membrane interface, as it mainly interacts electrostatically with the vesicle surface. In contrast, the W-E2(279–298) peptide is able to penetrate into negatively charged bilayers remaining close to the lipid/water interface. This nonpolar environment induces a peptide structural transi-

tion from random coil to α-helix, causing bilayer perturbations that lead to vesicle permeabilization.

In summary, our data suggest that the internal region (279–298) of the E2 structural protein may be involved in the fusion process of HGV/GBV-C.

Experimental procedures

Materials

Egg yolk PtdCho, brain PtdSer, PamOlePtdCho, PamOlePtdGro, 1-palmitoyl-2-stearoyl-(6–7)dibromo-*sn*-glycero-3-phosphocholine ($Br_{6,7}$-PtdCho) and 1-palmitoyl-2-stearoyl-(11–12)dibromo-*sn*-glycero-3-phosphocholine ($Br_{11,12}$-PtdCho) were from Avanti Polar Lipids (Alabaster, AL, USA). Calcein was from Fluka (Bucks, Switzerland). Rink amide MBHA and Novasyn TGR resins, amino-acid derivatives and coupling reagents were obtained from Fluka and Novabiochem (Nottingham, UK). Dimethylformamide was purchased from Sharlau (Barcelona, Spain). Trifluoroacetic acid was supplied by Merck (Poole, Dorset, UK) and scavengers such as ethanedithiol and tri-isopropylsilane were from Sigma-Aldrich (Steinheim, Germany).

Peptide synthesis

The peptides were synthesized manually following procedures described previously [23,24]. The syntheses were carried out by solid-phase methodology following an Fmoc/tBu strategy with a *N,N′*-di-isopropylcarbodiimide/1-hydroxybenzotriazole activation. For the incorporation of Cys293 into the E2(279–298) and W-E2(279–298) peptides, repeated coupling using 2-(1*H*-benzotriazol-1-yl)-1,1,3,3-tetramethyluronium tetrafluoroborate and *N,N′*-di-isopropylethylamine as activators was needed.

Threefold molar excesses of Fmoc-amino acids were used throughout the synthesis. The stepwise addition of each residue was determined by Kaiser's test [25]. Peptides were cleaved from the resin with a trifluoroacetic acid solution containing appropriate scavengers (either water and 1,2-ethanedithiol or water, tri-isopropylsilane ethanedithiol), and purified by HPLC on a semipreparative C_{18} kromasil column. The samples were eluted with a linear gradient of acetonitrile in an aqueous solution of 0.05% trifluoroacetic acid. Purified peptides were checked by analytical HPLC in an analytical C_{18} kromasil column, MALDI-TOF MS, and amino-acid analysis. Peptides were lyophilized and stored at 4 °C.

Positive control peptides

Penetratine(43–58) [26] and melittin [27] were used as positive control peptides throughout all the experimentation carried out. Penetratine(43–58) was used as a control in binding to SUVs, acrylamide quenching, brominated phospholipid quenching, and CD experiments. Melittin was used as a control in the leakage experiments.

Vesicle preparation

Lipid films were prepared by dissolving the phospholipids in a chloroform/methanol (2/1, v/v) solution, followed by solvent evaporation under a flow of nitrogen and overnight vacuum. Multilamellar vesicles were obtained by vortex mixing of the lipid films in 10 mM Tris/HCl buffer, pH 8.0, containing 0.15 M NaCl for 10 min above the phase transition temperature. On the one hand, SUVs were then obtained by sonication of the multilamellar vesicles at 4 °C using a Sonics Material Vibra-Cell™ sonicator. Titanium debris was removed by centrifugation. SUVs were separated from multilamellar vesicles by gel filtration on a Sepharose CL 4B column. The top fractions of the SUVs peak were pooled, concentrated and stored at 4 °C. On the other hand, LUVs were prepared by freeze-thawing the multilamellar vesicles in liquid nitrogen (15 times) [28], and extrusion through two stacked 100-nm polycarbonate filters (15 times; Nucleopore, Pleasanton, CA, USA) in a high-pressure extruder (Lipex Biomembranes, Vancouver, Canada) and stored at 4 °C.

PtdCho concentration was determined by an enzymatic colorimetric assay (bioMérieux), and total phospholipid concentration was determined by phosphorus analysis [29].

Trp fluorescence titrations

Fluorescence titrations were performed on an Aminco Bowman series 2 spectrofluorimeter, equipped with a thermostatically controlled cuvette holder (22 °C). Fluorescence emission spectra of 2 μM peptide solutions in 10 mM Tris/HCl containing 0.15 M NaCl, pH 8.0, in either the absence or presence of lipids, were recorded between 310 nm and 450 nm, with an excitation wavelength of 290 nm, at a slit width of 4 nm. The fluorescence spectra were instrument corrected for light scattering, by subtracting the corresponding spectra of the SUVs.

Changes in Trp fluorescence were used to evaluate peptide-lipid binding. The apparent dissociation constants were calculated from plots of the fluorescence intensity at 350 nm, expressed as the percentage of the fluorescence of the lipid-free peptides vs. the added lipid concentration. The data were analysed using Graphpad software, by means of the following equation:

$$F = \{F_0 + F_1(1/K_d)[L_{tot}]\}/\{1 + (1/K_d)[L_{tot}]\} \qquad (1)$$

where F is the fluorescence intensity at a given added lipid concentration, F_0 the fluorescence intensity at the beginning of the titration, F_1 the fluorescence at the end of the titration, K_d the dissociation constant, and $[L_{tot}]$ the total lipid concentration [30].

CD measurements

CD was measured on a Jasco 710 spectropolarimeter (Hachioji, Tokyo, Japan) between 184 and 260 nm in a quartz cell with a path length of 0.1 cm. Nine spectra were recorded and averaged. The spectra of the lipid-free peptides were measured in sodium phosphate buffer (50 mg·mL^{-1}) or in the presence of increasing percentages of trifluoroethanol (25%, 50%, 75%). CD spectra of lipid-bound peptides at peptide to lipid molar ratios of 1 : 20 or 1 : 40 were recorded after 1 h incubation at room temperature. The spectra were corrected by subtraction of the spectrum of the SUVs alone {results are expressed as mean residue ellipticities $[\theta]_{MR}$ (degree.cm^2·dmol^{-1})}. The secondary structure of the peptides was obtained by curve-fitting, using the K2D and Contin programs by the Dichroweb® server at http://www.cryst.bbk.ac.uk7cdweb [31,32]. The helical content of the peptides was also calculated from the mean residue ellipticity at 222 nm [33].

Acrylamide quenching experiments

For acrylamide quenching experiments, an excitation wavelength of 290 nm was used. Aliquots of the water–soluble acrylamide (10 M stock solution) were added to 2 μM peptide in 10 mM Tris/HCl buffer, pH 8.0, in the absence or presence of SUVs. The lipid/peptide mixtures (molar ratio 50 : 1) were incubated for 30 min at room temperature before the measurements. Fluorescence intensities at 350 nm were monitored after each acrylamide addition at 25 °C. The values obtained were corrected for dilution, and the scatter contribution was derived from acrylamide titration of a vesicle blank. K_{sv}, which is a measure of the accessibility of Trp to acrylamide, was obtained from the slope of the plots of F_0/F vs. [quencher], where F_0 and F are the fluorescence intensities in the absence and presence of quencher, respectively [18,34]. As acrylamide does not partition significantly into membrane bilayers, the value of K_{sv} can be considered the fraction of the peptide residing in the surface of the bilayer as well as the amount of nonvesicle-associated free peptide.

Brominated lipid quenching experiments

Quenching of Trp by brominated phospholipids was performed to find the localization of this residue in bilayers [35,36]. Peptides (2 μM) were incubated for 30 min at 22 °C with a 50-fold molar excess of lipids in 10 mM Tris/HCl buffer, pH 8. Emission spectra were recorded between 310 and 450 nm with an excitation wavelength of 290 (± 4 nm). The quenching efficiency (F_0/F) was calculated by dividing the Trp fluorescence intensity of the peptide in the presence of egg PtdCho/brain PtdSer (60/40) SUVs (F_0), by the Trp fluorescence intensity of the peptide in the presence of dibromo-PtdCho/brain PtdSer (70/30) SUVs (F). F_0/F was compared for quenching by $Br_{6,7}$-PtdCho and $Br_{11,12}$-PtdCho lipid-phase quenchers.

Assay of calcein leakage

Dequenching of encapsulated calcein fluorescence resulting from the leakage of aqueous content out of LUVs was used to assess the vesicle leakage activity of the peptides. LUVs containing calcein were obtained by hydration of the dried film in 10 mM Tris/HCl buffer, pH 8.0, containing 70 mM calcein. LUVs were prepared as described above, and non-encapsulated calcein was removed by gel filtration on a Sephadex G-100 column. Calcein leakage out of LUVs (50 μM lipids) was measured after 15 min incubation at 22 °C in the same buffer as was used for the fluorescence titrations. Calcein fluorescence was measured at 520 nm, with an excitation of 490 nm and slit widths of 4 nm, of a 50-fold diluted 20 μL sample of the peptide/lipid incubation mixture containing 50 μM lipids. Leakage (%) was calculated using the following equation:

$$\%\,\text{Leakage} = ([F - F_0]/[F_{100} - F_0]) \times 100 \qquad (2)$$

where F_0 is the fluorescence intensity of LUVs alone, F, the fluorescence intensity after incubation with the peptide, and F_{100}, the fluorescence intensity after the addition of 10 μL 5% (v/v) Triton X-100.

Assay of vesicle aggregation

The ability of the peptides to induce vesicle aggregation was studied by monitoring the turbidity of a SUV suspension of egg PtdCho/brain PtdSer (60/40) (50 μM) at 436 nm over 1 h (22 °C) on an Uvikon 941 spectrophotometer (peptide lipid to molar ratios of 0.2 and 0.04).

Acknowledgements

This work was funded by grants BQU2003-05070-CO2-01/02 from the Ministerio de Ciencia y Tecnología (Spain) and a predoctoral grant awarded to C. L. We are very grateful to Dr B. Vanloo for helpful discussions.

References

1 Stapleton JT (2003) GB virus type C/hepatitis G virus. *Semin Liver Dis* **23**, 137–148.
2 Martin II, Ruysschaert J & Epand RM (1999) Role of the N-terminal peptides of viral envelope proteins in membrane fusion. *Adv Drug Deliv Rev* **38**, 233–255.
3 White JM (1990) Viral and cellular membrane fusion proteins. *Annu Rev Physiol* **52**, 675–697.

4 Nieva JL & Agirre A (2003) Are fusion peptides a good model to study viral cell fusion? *Biochim Biophys Acta* **1614**, 104–115.
5 Voisset C & Dubuisson J (2004) Functional hepatitis C virus envelope glycoproteins. *Biol Cell* **96**, 413–420.
6 Rey FA, Heinz FX, Mandl C, Kunz C & Harrison SC (1995) The envelope glycoprotein from tick-borne encephalitis virus at 2 Å resolution. *Nature* **375**, 291–298.
7 Allison SL, Schalich J, Stiasny K, Mandl CW & Heinz FX (2001) Mutational evidence for an internal fusion peptide in flavivirus envelope protein E. *J Virol* **75**, 4268–4275.
8 Yagnik AT, Lahm A, Meola A, Roccasecca RM, Ercole BB, Nicosia A & Tramontano A (2000) A model for the hepatitis C virus envelope glycoprotein E2. *Proteins* **40**, 355–366.
9 Robertson B, Myers G, Howard C, Brettin T, Bukh J, Gaschen B, Gojobori T, Maertens G, Mizokami M, Nainan O, Netesov S, Nishioka K, Shini T, Simmonds P, Smith D, Stuyver L & Weiner A (1998) Classification, nomenclature, and database development for hepatitis C virus (HCV) and related viruses: proposals for standardization. International committee on virus taxonomy. *Arch Virol* **143**, 2493–2503.
10 Delos SE, Gilbert JM & White JM (2000) The central proline of an internal viral fusion peptide serves two important roles. *J Virol* **74**, 1686–1693.
11 Monne M, Hermansson M & von Heijne G (1999) A turn propensity scale for transmembrane helices. *J Mol Biol* **288**, 141–145.
12 Monne M, Nilsson I, Elofsson A & von Heijne G (1999) Turns in transmembrane helices: determination of the minimal length of a 'helical hairpin' and derivation of a fine-grained turn propensity scale. *J Mol Biol* **293**, 807–814.
13 Orzaez M, Salgado J, Gimenez-Giner A, Perez-Paya E & Mingarro I (2004) Influence of proline residues in transmembrane helix packing. *J Mol Biol* **335**, 631–640.
14 Larios C, Busquets MA, Carilla J, Alsina MA & Haro I (2004) Effects of overlapping GB virus C/hepatitis G virus synthetic peptides on biomembrane models. *Langmuir* **20**, 11149–11160.
15 Contreras LM, Aranda FJ, Gavilanes F, Gonzalez-Ros JM & Villalain J (2001) Structure and interaction with membrane model systems of a peptide derived from the major epitope region of HIV protein gp41: implications on viral fusion mechanism. *Biochemistry* **40**, 3196–3207.
16 Oren Z, Ramesh J, Avrahami D, Suryaprakash N, Shai Y & Jelinek R (2002) Structures and mode of membrane interaction of a short alpha helical lytic peptide and its diastereomer determined by NMR, FTIR, and fluorescence spectroscopy. *Eur J Biochem* **269**, 3869–3880.
17 Surewicz WK & Epand RM (1984) Role of peptide structure in lipid–peptide interactions: a fluorescence study of the binding of pentagastrin-related pentapeptides to phospholipid vesicles. *Biochemistry* **23**, 6072–6077.
18 Lakowicz JR (1983) Principles of fluorescence spectroscopy. In *Principles of Fluorescence Spectroscopy*, pp. 257–301. Plenum Press, New York.
19 Plasencia I, Rivas L, Keough KM, Marsh D & Perez-Gil J (2004) The N-terminal segment of pulmonary surfactant lipopeptide SP-C has intrinsic propensity to interact with and perturb phospholipid bilayers. *Biochem J* **377**, 183–193.
20 Del Angel VD, Dupuis F, Mornon JP & Callebaut I (2002) Viral fusion peptides and identification of membrane-interacting segments. *Biochem Biophys Res Commun* **293**, 1153–1160.
21 Zhang L & Ghosh HP (1994) Characterization of the putative fusogenic domain in vesicular stomatitis virus glycoprotein G. *J Virol* **68**, 2186–2193.
22 Allison SL, Schalich J, Stiasny K, Mandl CW & Heinz FX (2001) Mutational evidence for an internal fusion peptide in flavivirus envelope protein E. *J Virol* **75**, 4268–4275.
23 Rojo N, Gomara MJ, Haro I & Alsina MA (2003) Lipophilic derivatization of synthetic peptides belonging to NS3 and E2 proteins of GB virus-C (hepatitis G virus) and its effect on the interaction with model lipid membranes. *J Peptide Res* **61**, 318–330.
24 Larios C, Espina M, Alsina MA & Haro I (2004) Interaction of three beta-interferon domains with liposomes and monolayers as model membranes. *Biophys Chem* **111**, 123–133.
25 Kaiser E, Colescott RL, Bossinger CD & Cook PI (1970) Color test for detection of free terminal amino groups in the solid-phase synthesis of peptides. *Anal Biochem* **34**, 595–598.
26 Thoren PE, Persson D, Esbjorner EK, Goksor M, Lincoln P & Norden B (2004) Membrane binding and translocation of cell-penetrating peptides. *Biochemistry* **43**, 3471–3489.
27 Benachir T & Lafleur M (1995) Study of vesicle leakage induced by melittin. *Biochim Biophys Acta* **1235**, 452–460.
28 Mayer LD, Hope MJ & Cullis PR (1986) Vesicles of variable sizes produced by a rapid extrusion procedure. *Biochim Biophys Acta* **858**, 161–168.
29 Bartlett GR (1958) Phosphorous assay in column chromatography. *J Biol Chem* **234**, 466–468.
30 Christiaens B, Symoens S, Verheyden S, Engelborghs Y, Joliot A, Prochiantz A, Vandekerckhove J, Rosseneu M, Vanloo B & Vanderheyden S (2002) Tryptophan fluorescence study of the interaction of penetratin peptides with model membranes. *Eur J Biochem* **269**, 2918–2926.
31 Lobley A, Whitmore L & Wallace BA (2002) DICHROWEB: an interactive website for the analysis of protein secondary structure from circular dichroism spectra. *Bioinformatics* **18**, 211–212.

32 Whitmore L & Wallace BA (2004) DICHROWEB, an online server for protein secondary structure analyses from circular dichroism spectroscopic data. *Nucleic Acids Res* **32**, W668–W673.
33 Chen YH, Yang JT & Martinez HM (1972) Determination of the secondary structures of proteins by circular dichroism and optical rotatory dispersion. *Biochemistry* **11**, 4120–4131.
34 Eftink MR & Ghiron CA (1976) Exposure of tryptophanyl residues in proteins. Quantitative determination by fluorescence quenching studies. *Biochemistry* **15**, 672–680.
35 De Kroon AI, Soekarjo MW, De Gier J & De Kruijff B (1990) The role of charge and hydrophobicity in peptide–lipid interaction: a comparative study based on tryptophan fluorescence measurements combined with the use of aqueous and hydrophobic quenchers. *Biochemistry* **29**, 8229–8240.
36 Bolen EJ & Holloway PW (1990) Quenching of tryptophan fluorescence by brominated phospholipid. *Biochemistry* **29**, 9638–9643.